

Improbability of Void Growth in Aluminum via Dislocation Nucleation under Typical Laboratory Conditions

L. D. Nguyen¹ and D. H. Warner^{2,*}

¹*School of Applied and Engineering Physics, Cornell University, Ithaca, New York 14853, USA*

²*School of Civil and Environmental Engineering, Cornell University, Ithaca, New York 14853, USA*

(Received 4 August 2011; published 19 January 2012)

The rate at which dislocations nucleate from spherical voids subjected to shear loading is predicted from atomistic simulation. By employing the latest version of the finite temperature string method, a variational transition state theory approach can be utilized, enabling atomistic predictions at ordinary laboratory time scales, loads, and temperatures. The simulation results, in conjunction with a continuum model, show that the deformation and growth of voids in Al are not likely to occur via dislocation nucleation under typical loadings regardless of void size.

DOI: 10.1103/PhysRevLett.108.035501

PACS numbers: 61.72.Qq, 61.72.Bb, 62.20.fq, 62.20.M-

The failure of many modern engineering alloys is controlled by the growth and coalescence of internal voids. At high temperatures, void growth is thought to occur via diffusion, while at lower temperatures, shorter times, and/or higher loads, void growth is often attributed to dislocation plasticity. The plastic growth of large voids (tens of microns) is scale-independent and can accurately be described by traditional continuum plasticity theory, with the void size being sufficiently larger than the length scales of dislocation plasticity. Popular engineering fracture models are formulated upon this foundation [1,2]. The plastic growth of smaller voids is dependent upon their size, with the length scale of the stress or strain perturbation created by the void being on the order of the mobile dislocation and dislocation source spacing. Accordingly, the plastic growth of smaller voids must be described by using scale-dependent plasticity theories [3,4] (or discrete dislocation simulations [5,6]) to capture the smaller \rightarrow stronger trend observed in experiment [7,8]. The smallest voids, having nanometer dimensions, produce stress perturbations that interact with at most a few mobile dislocations and dislocation sources. Consequently, the growth of nanovoids is thought to depend upon the nucleation of dislocations from their surface. A large literature investigating this process has developed in the past decade.

Continuum analyses of dislocation nucleation from voids have been conducted by several independent research groups, e.g., [8–14]. The athermal analyses unanimously suggest that dislocation nucleation from the surface of a void is viable under very high loads. However, the qualitative insight offered by such analyses is limited in that significant geometric and parametric assumptions are often employed to make the analyses analytically tractable. Considering the nanoscale dimensions of the problem, atomistic simulations can provide a powerful investigative tool. In accordance with the continuum analyses, the simulations suggest that dislocation nucleation from voids is possible at very high loads and

short time scales [10,15–22]. This is consistent with post-testing microscopy in laser-shocked Cu (~ 5 GPa for ~ 10 ns) [23]. However, the plausibility of dislocation nucleation from voids under ordinary laboratory loads and longer time scales, where thermal activation can play a significant role, remains unclear. Here, we explore this question by using a newly developed atomistic simulation technique that enables the accurate calculation of finite temperature nucleation rates at time scales well beyond those accessible to standard molecular dynamics (MD) simulations.

Specifically, dislocation nucleation under ordinary experimental conditions is investigated with atomistic resolution in a variational transition state theory (V-TST) framework using the latest version of the finite temperature string method [24]. Both the V-TST approach and the Al interatomic potential [25] used here have recently been shown to accurately predict dislocation nucleation relative to direct MD and electronic structure simulations [26,27]. Nucleation from several nanovoid sizes and a free surface is examined at several loads. The results are then used as fitting data for a continuum model to provide predictions of dislocation nucleation rates across a range of meaningful void sizes and loads.

The V-TST framework provides a means to predict the rate at which a thermally activated event, such as dislocation nucleation, will occur [26,28,29]:

$$k = \sqrt{\frac{k_B T}{2m\pi}} Z_a^{-1} \int_{S_D} e^{-V(\bar{x})/k_B T} d\bar{s}(\bar{x}), \quad (1)$$

with k_B being the Boltzmann constant, T the temperature, m the effective mass, $V(\bar{x})$ the potential energy of the system in configuration \bar{x} , and $Z_a = \int_a e^{-V(\bar{x})/k_B T} d\bar{x}$ the configurational partition function over a . $\int_{S_D} d\bar{s}(\bar{x})$ represents an integral over a surface in configuration space, which in this case separates the set of unnucleated configurations from nucleated configurations. The term

“variational” denotes the fact that S_D is chosen to minimize the total frequency of transitions between the un-nucleated and nucleated states, $\nu_{\text{tot}}^{\text{freq}} = 2k p_{\text{un}}$, with p_{un} being the probability that the system exists in an un-nucleated configuration.

The primary challenge in obtaining a V-TST rate prediction is the computation of the integrals in Eq. (1). For this, we use a parallel implementation of the finite temperature string method [24]. The method is built upon a set of points in configuration space, which define a curve connecting an un-nucleated and nucleated configuration. Voronoi cells are defined about each point in configuration space, and the configuration space within each cell is sampled via independent simulations at 300 K. The cell centers are iteratively adjusted until they represent the average configuration associated with the sampling within each cell subject to an equal cell center spacing constraint. After the positions of the cell centers converge, the relative probability for the system to exist in each cell can be obtained by tabulating the frequency at which the simulations attempt to sample configurations in neighboring cells. By limiting the selection of the dividing surface S_D to the set of hyperplanes perpendicular to the string, the ratio of configuration space integrals in Eq. (1) can then be approximated as

$$Z_a^{-1} \int_{S_D} e^{-V(\bar{x})/k_B T} d\bar{s}(\bar{x}) \approx \frac{f_i}{\sum_{j=0}^i f_j w_j}, \quad (2)$$

where i represents the cell that straddles a particular choice of S_D , w_i the spacing between the cell walls of i along the string, and f_i the probability that the system is in cell i . The sampling of the atomistic configuration space was performed in the overdamped limit [24] by using a modified version of the LAMMPS package [30] and an Al embedded atom potential [25]. Between 30 and 100 cells were used in the calculations with a typical cell width of ~ 0.5 Å. The overall string length was held fixed, enabling a nonequilibrium nucleated configuration to be used for the end cell.

Three nanovoids of diameters $D = 4$ nm, $D = 6$ nm, and $D = 8$ nm and a faceted Al surface were examined. The specimens were strained in shear by adjusting the shape of the fully periodic cell (Fig. 1). The fcc lattice constant and unloaded cell dimensions corresponded to a zero pressure equilibrium state with $a_0^{300\text{K}} = 4.065$ Å. The crystallography and loading direction were chosen to provide the limiting case, i.e., most favorable for nucleation. The cells were composed of between 191 000 and 325 000 atoms such that the distance between free surfaces remained constant. To break the symmetry of the cell and provide a single preferred nucleation site, a few surface atoms were removed at one of the two peak shear stress locations. This did not have a significant ($< 7\%$) effect on the critical shear load at which instantaneous (less than a few picoseconds) nucleation occurred. The influence of the facets in the free surface simulation was examined at 0 K,

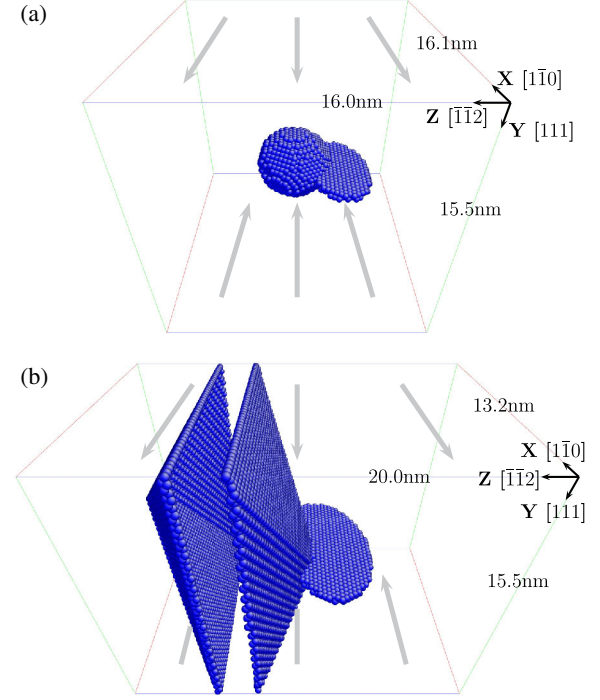


FIG. 1 (color online). Images of simulation cell geometries and loadings. (a) and (b) represent the $D = 4$ nm spherical void and faceted surface specimens at applied loads of 1.7 and 1.6 GPa, respectively. In both cases, the configurations represent the activated states, which involve only leading partial dislocations. The atoms in perfect fcc stacking are not shown [37]. Accordingly, the atoms shown in (a) depict the surface of the void and the stacking fault associated with the nucleating partial dislocation loop and in (b) depict the pair of Al surfaces and the stacking fault associated with the nucleating partial dislocation loop [37].

where the athermal nucleation stress was found to be 3% lower than the critical stress in an analogous simulation with no facets, i.e., a flat $[112]$ surface.

Standard NVT MD simulations were performed to determine the critical loads and to acquire the configurations needed to initialize the string. The simulations were conducted with a 1 fs time step at 300 K using a Langevin thermostat with a damping parameter of 1 ps [31]. The critical shear loads were found to be 2.16, 1.89, 1.70, and 1.90 GPa for the voids of diameter $D = 4$ nm, $D = 6$ nm, $D = 8$ nm, and the faceted surface, respectively. Nucleation from the faceted surface can be interpreted as nucleation from a spherical void with $D \rightarrow \infty$ by dividing the applied loading τ by the shear stress concentration factor of 1.87 [32], giving $\tau_{\text{crit}} = 1.02$ GPa for $D \rightarrow \infty$. The smaller \rightarrow stronger size effect observed here can be understood by considering that the finite size of the emerging dislocation core is acted upon by a force (stress \times area) that is dependent upon the size of the void [9,13,14].

In Fig. 2(a), the direct MD critical load predictions are given with the V-TST predictions at subcritical loads for two void sizes and the faceted surface. The nucleation rate

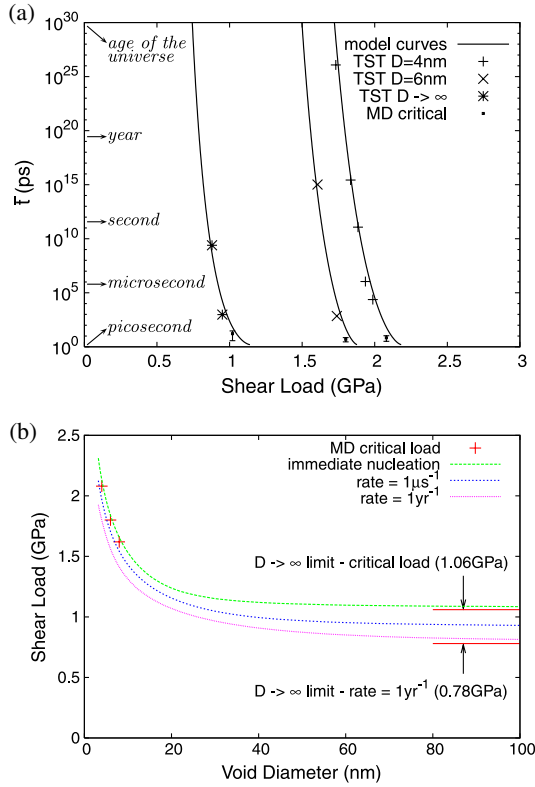


FIG. 2 (color online). (a) The expectation time for dislocation nucleation from a spherical void versus applied shear stress. The picoseconds data points were computed by using direct MD, while the points corresponding to longer times were computed with V-TST. The vertical bars on the MD data points correspond to the standard deviation of nucleation times collected from 50 independent simulations. (b) The applied shear stress required to achieve the specified nucleation rate as a function of spherical void size.

is found to quickly go to zero as the load is decreased from the critical load. The strong dependence on load is indicative of the process having a relatively large activation volume and is in accordance with the expected dividing surface configurations (activated state) shown in Fig. 1. The presence of a significantly sized dislocation loop and stacking fault area in the activated state (but not in the initial state) is the key feature that necessitates the use of advanced TST approaches, e.g., V-TST, as opposed to more approximate TST approaches, e.g., harmonic TST. Specifically, the presence of a large temperature-dependent defect only in the activated state can create a significant difference between the free energy and potential energy profiles along the reaction coordinate (Fig. 3). Differences in both the energy barrier height and position become more significant with decreasing load, as the dislocation loop in the activated state becomes larger. This finding is consistent with two recently published works that have highlighted the importance of considering the free energy profile when predicting dislocation nucleation [26,33].

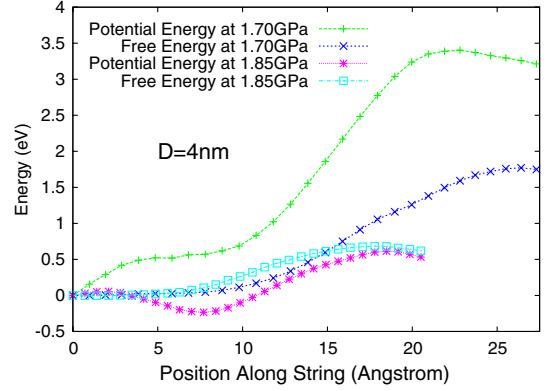


FIG. 3 (color online). The potential and free energy profiles along the 300 K principle curves [24] (strings) associated with partial dislocation nucleation from a spherical void at two fixed loadings. The considerable difference between the curves highlights the importance of entropy and indicates that the position of the principle curve in configuration space is significantly dependent upon load.

To obtain predictions of dislocation nucleation rates across a range of meaningful void sizes and applied loads, the simulation data points were interpolated or extrapolated by using an isotropic elastic continuum model that provided physical guidance. For our purpose, the specific details of the model have little consequence on the final conclusions. The model was constructed from an Arrhenius perspective of nucleation rates, where the expectation time for nucleation is written as $\bar{t} = \nu_0^{\text{freq}^{-1}} \exp(\Delta E^{\text{total}}/k_B T)$. ΔE^{total} represents the change in energy associated with the nucleating partial dislocation growing from its small equilibrium configuration to the nearby saddle configuration.

For simplicity, the nucleating dislocation segment was assumed to have a constant radius of curvature r and consist of three distinct energy components: $E^{\text{total}} = E^{\text{ssf}} + E^{\text{disl}} - W^{\text{stress}}$. E^{ssf} represents the energy of the stable stacking fault created by the partial dislocation segment, $E^{\text{ssf}} = \gamma_{\text{ssf}} A$, where A is the area swept by the nucleating dislocation segment. W^{stress} represents the interaction of the dislocation with the stress field created by the applied load, $W^{\text{stress}} = \int_A b_p^s \tau_{xy} ds$, where τ_{xy} corresponds to the xy shear stress field on the slip plane due to the applied load. The expression for τ_{xy} in an infinite elastic body containing a void is lengthy; thus, we refer interested readers to Ref. [32] for brevity. b_p^s corresponds to the magnitude of the partial Burgers vector in the $[1\bar{1}0]$ direction. E^{disl} represents the self-energy of the nucleating dislocation segment and was taken to be

$$E^{\text{disl}} = \frac{\mu b_p^2 r}{8} \frac{2 - \nu}{1 - \nu} \ln\left(\frac{4gr}{e^2 r_0}\right), \quad (3)$$

with μ being the shear modulus, b_p the magnitude of the partial dislocation Burgers vector, ν the Poisson's ratio,

and r_0 the dislocation core cutoff radius. The function g captures the influence of void diameter D on the dislocation self-energy:

$$g = 0.55 + \frac{\frac{4r}{e^2 r_0} - 0.55}{1 + \alpha(D)/r}. \quad (4)$$

The form of g was chosen such that E^{disl} corresponds to the available analytic solutions for the two limiting cases of $r/D \rightarrow \infty$ (a full dislocation loop in an infinite elastic material [34]) and $r/D \rightarrow 0$ (a half dislocation loop at a free surface [35]). $\alpha(D)$ controls the rate at which E^{disl} transitions between these two solutions and was taken to be $\alpha(D) = c_2 D^2 + c_1 D$. By using $\mu = 69$ GPa, $\nu = 0.33$, $r_0 = 1.1$ Å, $b_p = 1.65$ Å, $\gamma_{\text{ssf}} = 0.118$ J/m², and $\nu_0^{\text{freq}} = 0.62$ ps⁻¹, the continuum model was fit to the atomistic results for the $D = 4$ nm and $D = 6$ nm voids by setting $c_1 = 0.217$ and $c_2 = 0.079$ nm⁻¹. The performance of the fit is demonstrated by its closeness with the atomistic simulation data for the $D \rightarrow \infty$ and $D = 8$ nm data in Fig. 2.

Together, the atomistic simulations and analytic model suggest that dislocation nucleation will occur from spherical voids at far-field shear loadings of 0.9–2.0 GPa at 300 K depending upon the void size ($D > 4$ nm) and the time scale ($\bar{t} < 1$ yr), as shown in Fig. 2(b). For large voids, with diameters greater than 100 nm, the nucleation load can be considered independent of size. For any particular void size, nucleation is highly unlikely at loads below $\sim 75\%$ of the critical load. Considering that all technologically relevant Al alloys have ultimate tensile strengths below 1 GPa, the nucleation of dislocations from voids is predicted to be highly unlikely, unless the material is subjected to extreme shock loading [23] or voids are subjected to nanoscale stress concentrations such as other nearby dislocations.

With regard to mechanical testing, if dislocation nucleation from voids were to occur, the predictions suggest that the response would be considered relatively strain rate insensitive. Specifically, the strain rate sensitivity $m = \partial \ln \tau_f / \partial \ln \dot{\gamma}$, associated with a material whose deformation is completely controlled by the nucleation of dislocations from voids, $\dot{\gamma} \propto k$, is predicted to be 0.004 at typical experimental time scales, with $\dot{\gamma}$ representing the shear strain rate and τ_f the shear flow strength. While this value is relatively independent of void size, it does depend upon the load or time scale at high ($> \text{ms}^{-1}$) nucleation rates, e.g., $m \approx 0.012$ at typical molecular dynamics rates (ns⁻¹). As a point of reference, mechanical testing of coarse-grained polycrystalline Al, where deformation is controlled by dislocation-dislocation interactions, exhibits $m \approx 0.004$ [36].

In summary, we have combined atomistic modeling, variational TST, and a simple analytic model to predict dislocation nucleation rates from a spherical void in Al. Our findings suggest that nucleation is unlikely to occur

under ordinary experimental conditions. This not only contributes to the ongoing debate regarding the mechanisms of nanovoid growth and ductile failure [5–10,13–20,23] but also provides a prediction of the maximum attainable strength of Al alloys.

The authors acknowledge support from Paul Hess at ONR (Grants No. N00014-08-1-0862 and No. N00014-10-1-0323).

*dhw52@cornell.edu

- [1] A. L. Gurson, *J. Eng. Mater. Technol.* **99**, 2 (1977).
- [2] J. R. Rice and D. M. Tracey, *J. Mech. Phys. Solids* **17**, 201 (1969).
- [3] N. A. Fleck and J. W. Hutchinson, *J. Mech. Phys. Solids* **41**, 1825 (1993).
- [4] S. S. Chakravarthy and W. A. Curtin, *Proc. Natl. Acad. Sci. U.S.A.* **108**, 15716 (2011).
- [5] M. Huang, Z. Li, and C. Wang, *Acta Mater.* **55**, 1387 (2007).
- [6] J. Segurado and J. Llorca, *Acta Mater.* **57**, 1427 (2009).
- [7] M. B. Taylor, H. M. Zbib, and M. A. Khaleel, *Int. J. Plast.* **18**, 415 (2002).
- [8] D. C. Ahn, P. Sofronis, M. Kumar, J. Belak, and R. Minich, *J. Appl. Phys.* **101**, 063514 (2007).
- [9] D. Ahn, P. Sofronis, and R. Minich, *J. Mech. Phys. Solids* **54**, 735 (2006).
- [10] T. Tsuru and Y. Shibutani, *J. Phys. D* **40**, 2183 (2007).
- [11] T. C. Tzeng, *J. Appl. Phys.* **103**, 053509 (2008).
- [12] F. D. Fischer and T. Antretter, *Int. J. Plast.* **25**, 1819 (2009).
- [13] V. A. Lubarda, *Int. J. Plast.* **27**, 181 (2011).
- [14] L. Wang, J. Zhou, Y. Liu, S. Zhang, Y. Wang, and W. Xing, *Mater. Sci. Eng. A* **528**, 5428 (2011).
- [15] E. T. Seppala, J. Belak, and R. E. Rudd, *Phys. Rev. B* **69**, 134101 (2004).
- [16] E. T. Seppala, J. Belak, and R. E. Rudd, *Phys. Rev. B* **71**, 064112 (2005).
- [17] J. Marian, J. Knap, and M. Ortiz, *Phys. Rev. Lett.* **93**, 165503 (2004).
- [18] J. Marian, J. Knap, and M. Ortiz, *Acta Mater.* **53**, 2893 (2005).
- [19] G. P. Potirniche, M. F. Horstemeyer, G. J. Wagner, and P. M. Gullett, *Int. J. Plast.* **22**, 257 (2006).
- [20] S. Traiviratana, E. M. Bringa, D. J. Benson, and M. A. Meyers, *Acta Mater.* **56**, 3874 (2008).
- [21] K. J. Zhao, C. Q. Chen, Y. P. Shen, and T. J. Lu, *Comput. Mater. Sci.* **46**, 749 (2009).
- [22] E. M. Bringa, S. Traiviratana, and M. A. Meyers, *Acta Mater.* **58**, 4458 (2010).
- [23] V. A. Lubarda, M. S. Schneider, D. H. Kalantar, B. A. Remington, and M. A. Meyers, *Acta Mater.* **52**, 1397 (2004).
- [24] E. Vanden-Eijnden and M. Venturoli, *J. Chem. Phys.* **130**, 194103 (2009).
- [25] Y. Mishin, D. Farkas, M. J. Mehl, and D. A. Papaconstantopoulos, *Phys. Rev. B* **59**, 3393 (1999).
- [26] L. D. Nguyen, K. L. Baker, and D. H. Warner, *Phys. Rev. B* **84**, 024118 (2011).

- [27] A. K. Nair, D. H. Warner, R. G. Hennig, and W. A. Curtin, *Scr. Mater.* **63**, 1212 (2010).
- [28] E. Vanden-Eijnden and F. A. Tal, *J. Chem. Phys.* **123**, 184103 (2005).
- [29] J. Horiuti, *Bull. Chem. Soc. Jpn.* **13**, 210 (1938).
- [30] S. Plimpton, *J. Comput. Phys.* **117**, 1 (1995).
- [31] T. Schneider and E. Stoll, *Phys. Rev. B* **17**, 1302 (1978).
- [32] L. He and Z. Li, *Int. J. Solids Struct.* **43**, 6208 (2006).
- [33] S. Ryu, K. Kang, and W. Cai, *Proc. Natl. Acad. Sci. U.S.A.* **108**, 5174 (2011).
- [34] J. P. Hirth and J. Lothe, *Theory of Dislocations* (McGraw-Hill, New York, 1968).
- [35] G. E. Beltz and L. B. Freund, *Phys. Status Solidi B* **180**, 303 (1993).
- [36] J. May, H. Hoppel, and M. Goken, *Scr. Mater.* **53**, 189 (2005).
- [37] J. Li, *Model. Simul. Mater. Sci. Eng.* **11**, 173 (2003).